Supporting Information

Light Processing Enables Efficient Carbon-Based, All-Inorganic Planar $CsPbIBr_2$ Solar Cells with High Photovoltages

Qianni Zhang,[#] Weidong Zhu,[#,*] Dazheng Chen, Zeyang Zhang, Zhenhua Lin, Jingjing Chang, Jincheng Zhang, Chunfu Zhang,[*] and Yue Hao

State Key Discipline Laboratory of Wide Band Gap Semiconductor Technology & Shaanxi Joint Key Laboratory of Graphene, School of Microelectronics, Xidian University, Xi'an, 710071, China.

[#]*These authors contribute equally to the work.*

[*]*Address correspondence to wdzhu@xidian.edu.cn and cfzhang@xidian.edu.cn*

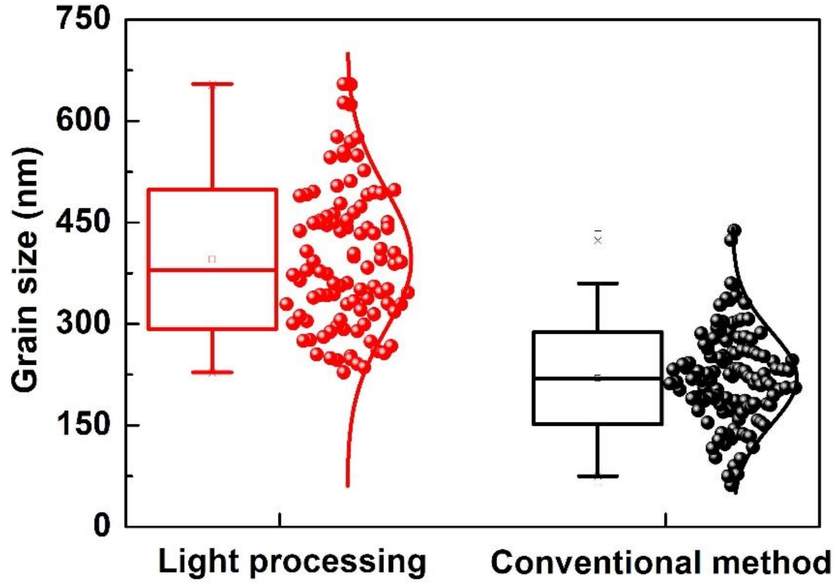

Figure S1. Statistic grain sizes distributions in the $CsPbIBr_2$ films prepared by light processing and conventional method, respectively.

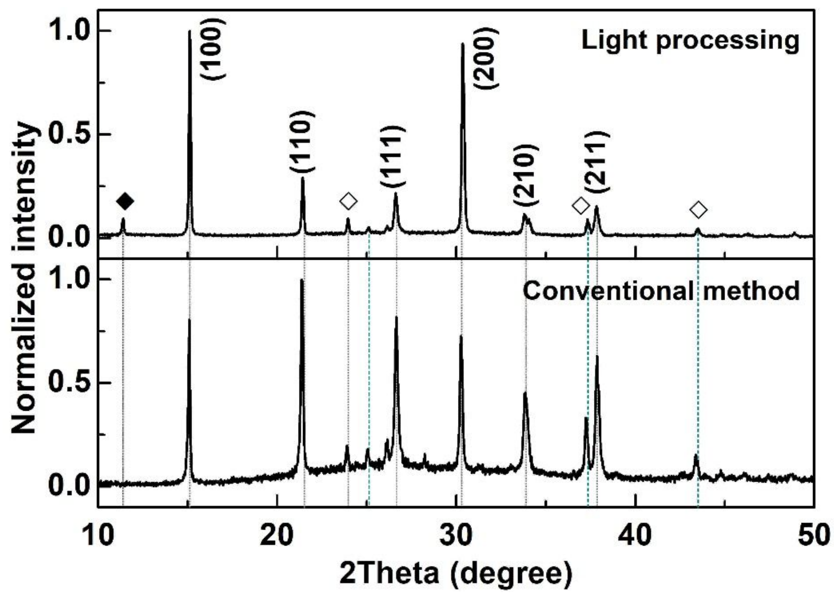

Figure S2. Normalized XRD patterns of $CsPbIBr_2$ films formed by light processing and conventional method, respectively. The symbols of solid diamond and open diamond represent the signals from $PbBr_2$ impurity phase and c-TiO_2/FTO substrate, respectively.

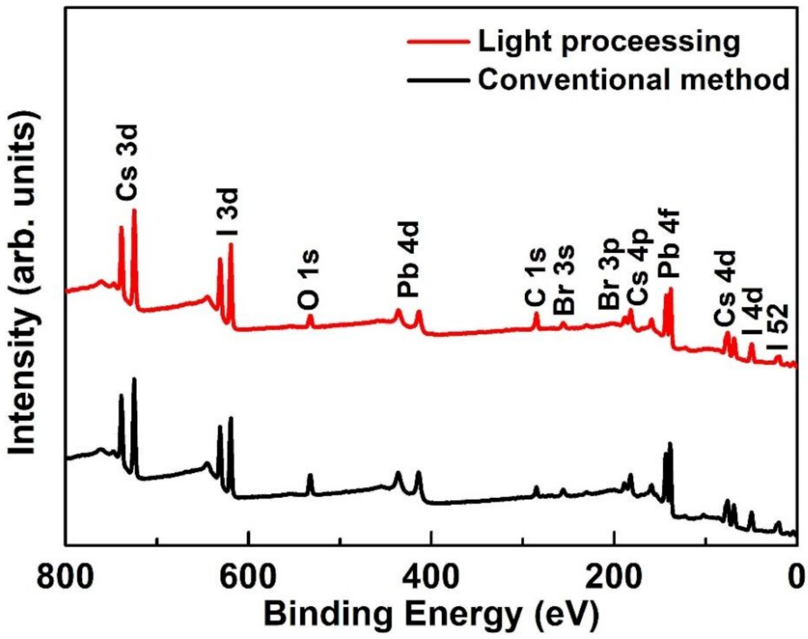

Figure S3. XPS survey spectra of $CsPbIBr_2$ films prepared by light processing and conventional method, respectively.

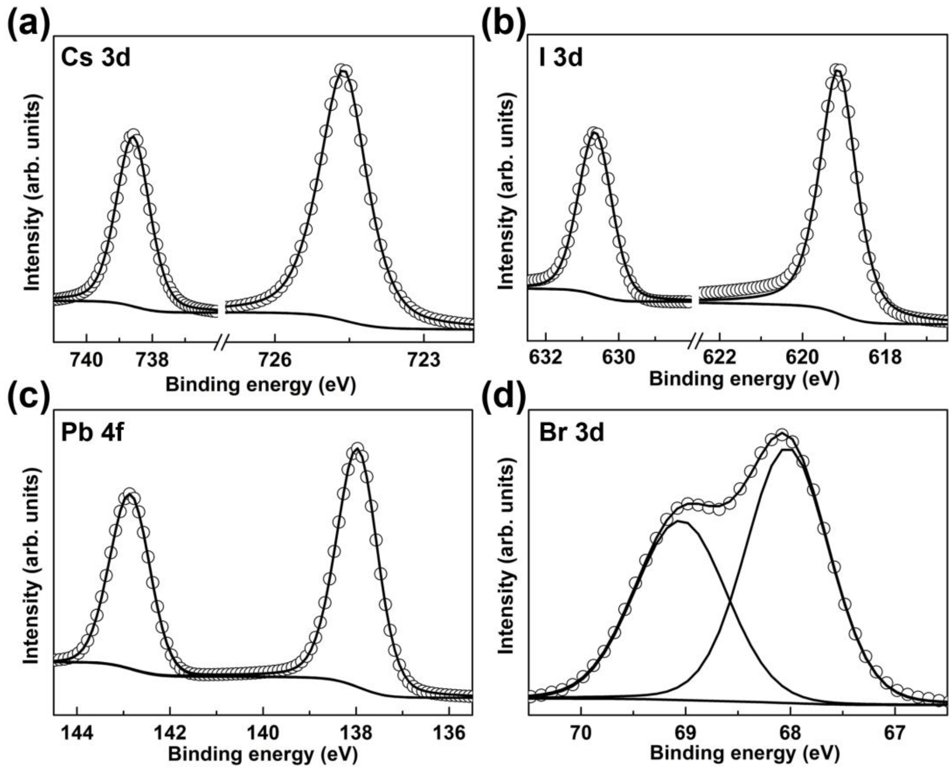

Figure S4. (a-d) Core-level XPS spectra of the $CsPbIBr_2$ film prepared by light processing after washing with absolute methanol.

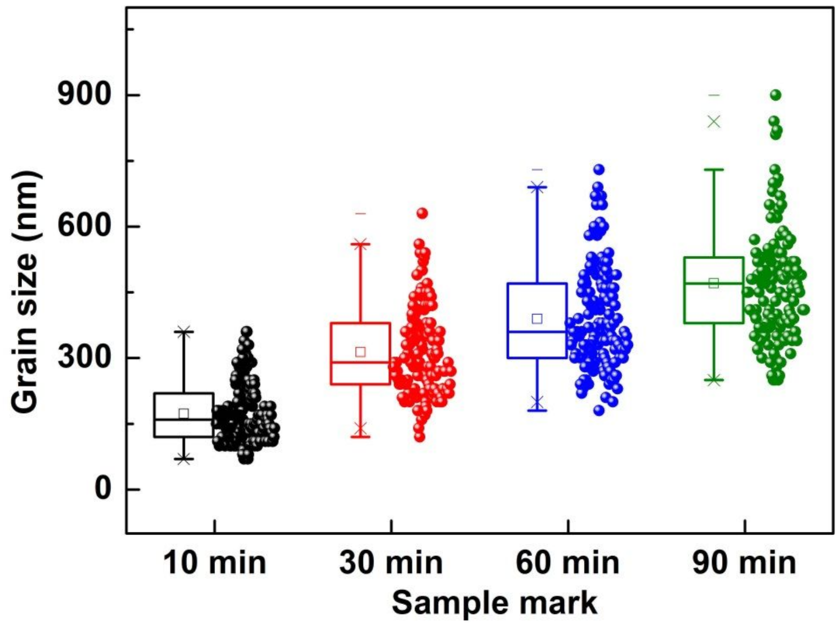

Figure S5. Statistic grain sizes distributions of the $CsPbIBr_2$ films with different light processing times of 10, 30, 60, and 90 min, respectively.

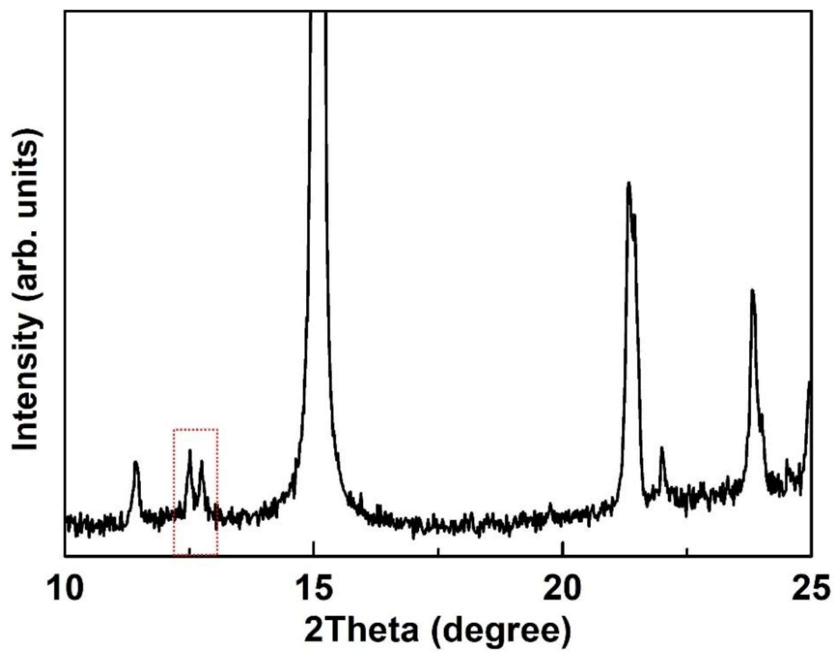

Figure S6. Enlarged XRD pattern of the $CsPbIBr_2$ film prepared by light processing with the time of 90 min. The red rectangle marks the signal from non-perovskite phase $CsPbIBr_2$.

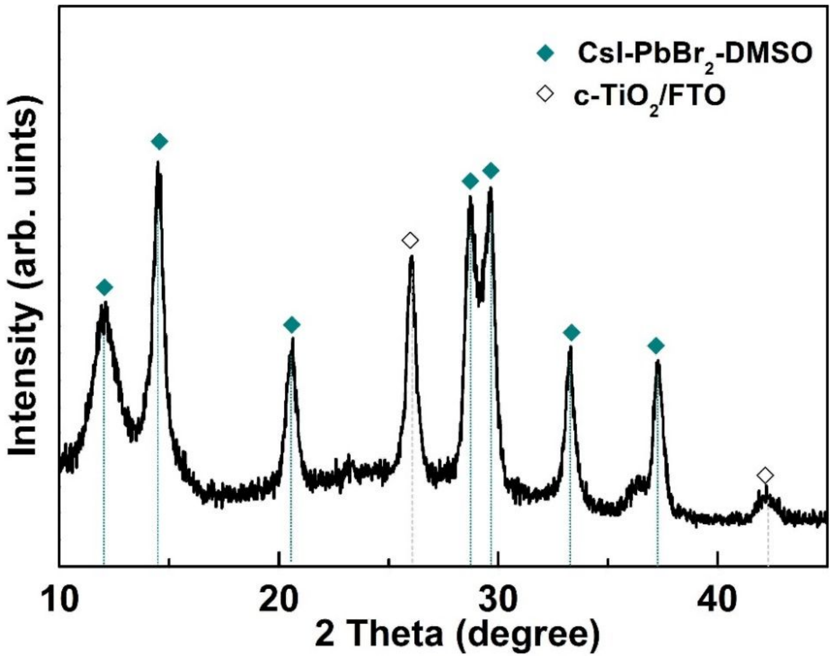

Figure S7. XRD pattern of the precursor $CsPbIBr_2$ film. It indicates that the film is composed of crystalline CsI-$PbBr_2$-DMSO intermediate phase.

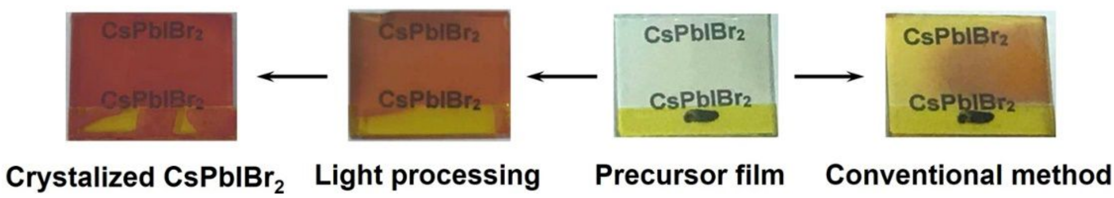

Figure S8. Optical images of the precursor $CsPbIBr_2$ film (Precursor film), the one after light processing (Light processing), and the one after being stored at 25 ^{o}C in dark for 60 min (Conventional method), as well as the ultimate $CsPbIBr_2$ film formed by light processing (Crystalized $CsPbIBr_2$), respectively.

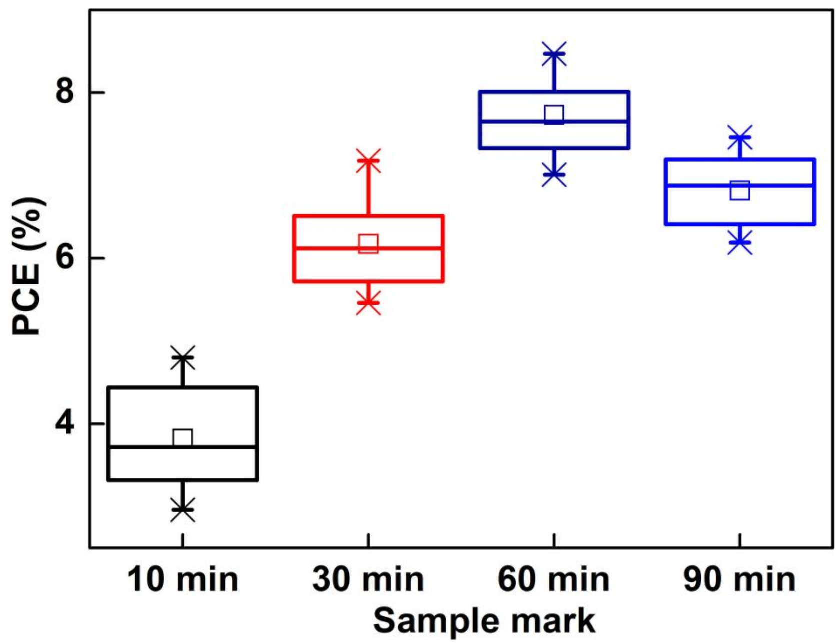

Figure S9. Statistic PCEs of 20 independent cells based on the $CsPbIBr_2$ films with different light processing times of 10, 30, 60, and 90 min, respectively.

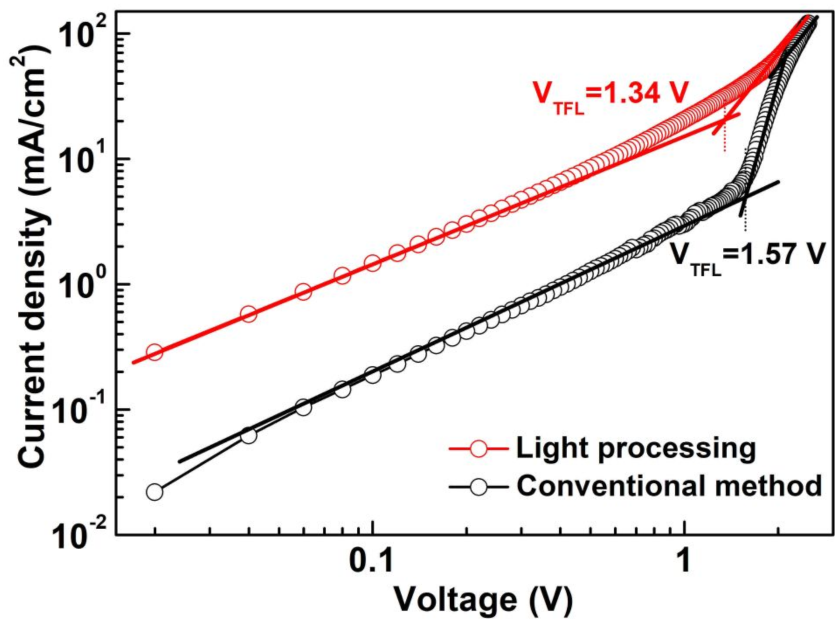

Figure S10. Hole-only dark J-V curves as well as the SCLC analyses for the $CsPbIBr_2$ films prepared by light processing and conventional method, respectively.

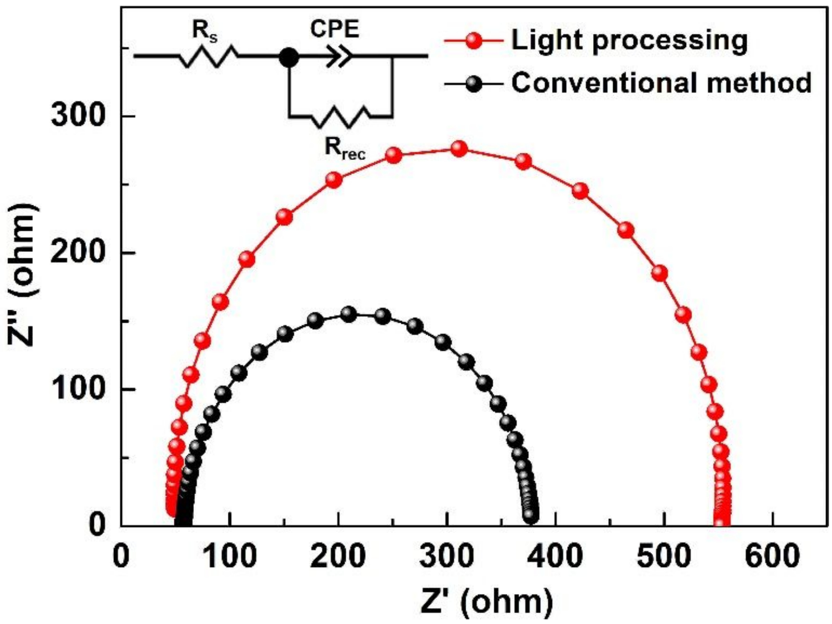

Figure S11. Fitted Nyquist plots for the cell fabricated by light processing and conventional method, respectively. The insert is the equivalent circuit for the fittings.

Table S1. Summary the E_{loss} values along with V_{oc} values and PCEs for pure $CsPbIBr_2$-based solar cells reported so far.

Cell configuration	E_g (eV)	V_{oc} (V)	PCE (%)	E_{loss} (eV)	Refs.
FTO/c-TiO_2/$CsPbIBr_2$/Carbon	2.05	1.245	9.16	0.805	[25]
ITO/SnO_2/$CsPbIBr_2$/ spiro-OMeTAD/Ag	2	1.15	8.54	0.85	[27]
FTO/c-TiO_2/m-TiO_2/$CsPbIBr_2$/Carbon	1.90	1.08	8.25	0.82	[22]
FTO/c-TiO_2/$CsPbIBr_2$/ spiro-OMeTAD/Au	2.05	1.227	8.02	0.823	[32]
ITO/SnO_2/C60/$CsPbIBr_2$/ spiro-OMeTAD/Au	2.04	1.18	7.34	0.86	[31]
FTO/c-TiO_2/$CsPbIBr_2$/Carbon	2.05	1.142	6.55	0.908	[24]
FTO/c-TiO_2/m-TiO_2/ $CsPbIBr_2$/spiro-OMeTAD/Au	2.05	1.121	6.30	0.929	[28]
FTO/c-TiO_2/m-TiO_2/$CsPbIBr_2$/Carbon	1.89	0.96	6.14	0.93	[23]
FTO/NiO_x/$CsPbIBr_2$/ZnO/Al	2.1	1.01	5.57	1.09	[34]
FTO/NiO_x/$CsPbIBr_2$/MoO_x/Au	2.08	0.85	5.52	1.23	[30]
ITO/ZnO/$CsPbIBr_2$/ spiro-OMeTAD/Ag	2.06	1.04	4.8	1.01	[33]
FTO/c-TiO_2/$CsPbIBr_2$/Au	2.05	0.959	4.70	1.091	[29]

Table S2. Compositional atom ratios in $CsPbIBr_2$ films obtained by light processing and conventional method, respectively, as well as that for the former after washing with absolute methanol.

Samples	Cs (at.%)	Pb (at.%)	I (at.%)	Br (at.%)	(Cs+I)/(Pb+Br/2)
Light processing	10.28	5.92	8.93	13.04	1.54
Conventional method	10.01	8.19	9.02	18.25	0.97
Light processing after washing	9.85	7.87	9.23	17.61	1.14

Table S3. Summary of photovoltaic parameters of pure $CsPbIBr_2$-based solar cells reported so far.

Cell configuration	V_{oc} (V)	J_{sc}(mA cm^{-2})	FF	PCE (%)	Refs.
FTO/c-TiO_2/m-TiO_2/$CsPbIBr_2$/Carbon	1.283	11.17	0.60	8.60	**This work**
FTO/c-TiO_2/$CsPbIBr_2$/Carbon	1.245	10.66	0.69	9.16	[25]
ITO/SnO_2/$CsPbIBr_2$/spiro-OMeTAD/Ag	1.15	10.61	0.70	8.54	[27]
FTO/c-TiO_2/m-TiO_2/$CsPbIBr_2$/Carbon	1.08	12.32	0.62	8.25	[22]
FTO/c-TiO_2/$CsPbIBr_2$/spiro-OMeTAD/Au	1.227	9.69	0.674	8.02	[32]
ITO/SnO_2/C60/$CsPbIBr_2$/spiro-OMeTAD/Au	1.18	8.32	74.8	7.34	[31]
FTO/c-TiO_2/$CsPbIBr_2$/Carbon	1.142	9.11	0.63	6.55	[24]
FTO/c-TiO_2/m-TiO_2/$CsPbIBr_2$/spiro-OMeTAD/Au	1.121	7.9	0.70	6.30	[28]
FTO/c-TiO_2/m-TiO_2/$CsPbIBr_2$/Carbon	0.96	12.15	0.53	6.14	[23]
FTO/NiO_x/$CsPbIBr_2$/ZnO/Al	1.01	8.65	0.636	5.57	[34]
FTO/NiO_x/$CsPbIBr_2$/MoO_x/Au	0.85	10.56	0.62	5.52	[30]
ITO/ZnO/$CsPbIBr_2$/spiro-OMeTAD/Ag	1.04	8.78	0.525	4.8	[33]
FTO/c-TiO_2/$CsPbIBr_2$/Au	0.959	8.7	0.56	4.70	[29]